

Alloy Design Strategies of the Native Anti-corrosion Magnesium Alloy

Tao Chen, Yuan Yuan, Jiajia Wu, Tingting Liu, Xianhua Chen, Aitao Tang, and Fusheng Pan

Abstract

Application of Mg alloy is limited because of its poor corrosion resistance. Due to low standard electrode potential of Mg, severe galvanic corrosion can happen if other alloyed elements form high electrode potential precipitate in Mg alloy. Moreover, natively formed oxide film on the surface of pure Mg is not compact and cannot hinder further oxidation of inner substrate. In this work, alloy design strategies are proposed to improve the native anti-corrosion property of Mg alloys. The first is to purify the Mg-melt by forming high-density precipitates in the settling process to increase the efficiency of the settling process. The second is to enclose extra impurities in harmless compounds to avoid the severe galvanic corrosion. The third is to control the composites of oxides formed on the surface by alloying defined elements to obtain passivate, close packing oxides film.

Keywords

Mg alloy • Anti-corrosion • Alloy design

Introduction

Magnesium is the lightest metal material among common structural metals and consider being energy-efficient. Therefore, magnesium alloys have attracted extensive attentions in transportation field [1–4]. However, abroad

applications of Mg alloys are limited due to their low ductility and native poor anti-corrosion property [5].

The poor anti-corrosion property of Mg is attributed to two major reasons [6, 7]. One reason is the naturally formed magnesium oxide film on its surface is not protective for further oxidation of inner substrate. The Pilling-Bedworth ratio (P-B ratio) of pure magnesium is 0.81. The natively formed oxide film on Mg alloy is not compact and is not able to hinder further oxidation [7]. Another reason is Mg has the lowest hydrogen evolution potential among common metals and severe galvanic corrosion often happens with magnesium alloy when other elements were alloyed in the alloy. Meanwhile, solubility of many metals (e.g., Fe, Ni, Cr, Cu [8–13]) in magnesium is very low (in the order of magnitude of ppm of weight fraction). Therefore, the impurities in Mg alloy are easy to precipitate and result in galvanic corrosion as formed galvanic couples with Mg substrate phases.

In the current work, three alloy design strategies of magnesium alloy are suggested to enhance the native corrosion resistance of Mg alloy.

Alloy Design Strategies

Purification of Mg-melt by Controlling Precipitates in Settling Process

Fe, Ni, Cu, and Cr have small solubility in the primary α (Mg) phase thus can precipitate as Mg–X compounds during its solidification process and cause severe galvanic corrosion. Many publications and patents were devoted to decrease the content of these impurities [13–25]. Among these impurities, Fe has attracted more attentions [18, 23, 26] as it is easy to be picked up during the synthesis process.

Among many purification methods, one approach is to let the precipitates settle down to the bottom. As illustrated in our previous work [27], the required fully settling time of precipitates is much longer than the usually applied settling process as half an hour by industry. Clearly, efficiency and

T. Chen · Y. Yuan (✉) · J. Wu · T. Liu · X. Chen
A. Tang · F. Pan

College of Materials Science and Engineering, Chongqing University, Chongqing 400000, China
e-mail: yuan yuan17@cqu.edu.cn

T. Chen · Y. Yuan · J. Wu · T. Liu · X. Chen · A. Tang · F. Pan
National Engineering Research Center for Magnesium Alloys,
Chongqing University, Chongqing 400000, China

Table 1 The terminal settling velocity of precipitates in Mg-melt

Alloy	T (°C)	Sol. of Fe in L (ppm in w.f.)	Precipitated particles	Comp. of prec. (at.%)	Density of pre.	v (m/s)	References
Mg	660	180	Bcc(Fe)	Fe	7.86	4.53e-5	This work
AZ91 without Mn	760	62	Bcc(Fe, Al)	Al50Fe50	5.61	3.6e-5	[27]
	730	36	Al ₂ Fe	Al67Fe33	4.08	2.1e-5	
	660	8	Al ₅ Fe ₂	Al5Fe2	3.96	1.7e-5	
AZ91 + 0.1 wt% Mn	730	35	Bcc(Fe, Al)	Al50Fe50	5.61	3.4e-5	[27]
	662	9	Al ₂ Fe	Al67Fe33	4.08	1.8e-5	
AZ91 + 0.3 wt% Mn	700	15	Al ₈ Mn ₅	Al54Fe16Mn30	4.00	2.2e-5	This work
	660	8	Al ₈ Mn ₅	Al54Fe16Mn30		2.0e-5	
Mg + Zr	700	2	Fe ₂ Zr	Fe66Zr34	7.65	4.9e-5	This work

Sol. of Fe in L (ppm in w.f.): Calculated solubility of Fe in Liquid (ppm in weight fraction) (The calculation is based on PanMg database)

Comp. of Prec.: The composition of the precipitates (experimental measured results)

v: The terminal settling velocity of the precipitates calculated using Stokes equation

effectiveness of the settling process is actually the determining factor of the final purity of the alloy.

According to Stokes Eq. (1), terminal velocity of different precipitates during settling process were calculated.

$$v = \frac{2gr(\Delta\rho)}{9\eta} \quad (1)$$

where $\Delta\rho$ denotes the difference of the densities of the particles and of the fluid, η denotes the viscosity of the fluid, g is the gravitational acceleration (9.8 m/s^2), and r is the radius of the spherical participation particles, which, according to our experimental measured results, is around $2 \mu\text{m}$.

Viscosity with temperature dependence of AZ91D magnesium alloy reported by Abaturvov [28] is employed as a general data for Mg-melt in this calculation.

As shown in Table 1 and Fig. 1, the addition of Mn does not change much on the solubility of Fe in the Mg-melt, but the precipitations on the defined temperature were changed. The terminal settling velocity relates to the density of the precipitate. With different precipitates, the terminal settling velocity can be quite different. Accordingly, the effectiveness of the settling process can be quite different in the limited settling period.

As shown in Table 1, with 0.1 wt% Mn addition, the Bcc (Fe) with Al solution can be stabilized up to 730 °C. At 730 °C, the terminal settling velocity of Bcc(Fe, Al) is $3.4e-5 \text{ m/s}$, 1.6 times of that of Al₂Fe. However, with more Mn addition, like 0.3 wt% Mn addition, the precipitation at 700 °C is changed to Al₈Mn₅ with Fe dissolved in Mn sublattice, which have low settling velocity again. It is consistent with the observation that too much Mn addition will deteriorate the anti-corrosion property of Magnesium alloy [29]. Calculated isopleth of AZ91 at 700 °C based on PanMg database is shown in Fig. 1.

According to Fig. 1, the suggested Mn addition is between 0.14 wt% and 0.27 wt% for AZ91 alloy. According to our calculation, terminal settling velocity of Fe₂Zr is even bigger if Zr is added in Mg melt. However, Zr will react Al and form Al₃Zr instead of Fe₂Zr with Al presence. Hence, the Zr additive is not recommended for the purification of Mg–Al–X series alloy.

Hence, by adding defined elements to control the type of the precipitates is an effective way to improve the efficiency of the settling process and, accordingly, improve the final purity level of the Mg alloy.

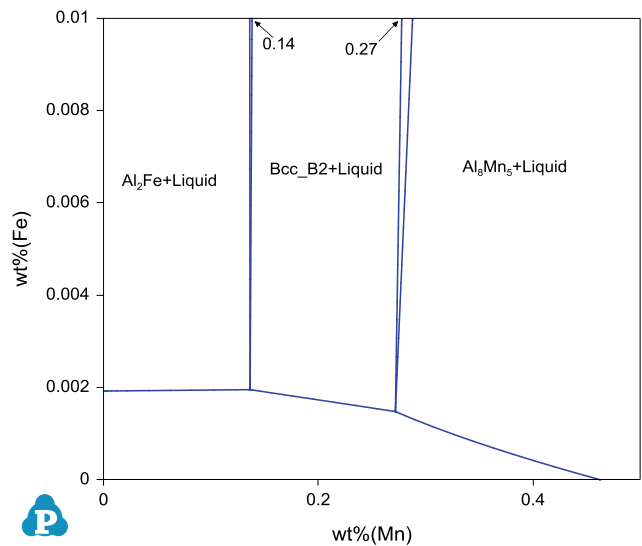


Fig. 1 Isothermal section of AZ91 with variation of Mn and Fe at 700 °C [27]

The Increasing of the Tolerance Limit of the Impurities by Controlling the Formed Precipitates in the Final Alloy

Another cost-efficient way to decrease the galvanic corrosion is to increase the tolerance limit of the impurities in Mg alloy.

It is observed the tolerance limit of Fe has a fixed ratio with the content of Mn in Mg alloy [8–11, 13]. The mechanism of Mn addition to increase the tolerance limit of Fe in Mg–Al–X alloy is illustrated in our previous work [27]. For Mg–Al–X alloy, addition of Mn can modify the precipitates in the final alloy and, therefore, change the distribution of Fe in different phases. When most of the extra Fe atoms are dissolved in compounds, which have less effect on the galvanic corrosion, no severe galvanic corrosion will happen to the Mg alloy. As reported in [27], the preferred formed phases in the alloys were Al–Mn compounds with Fe dissolved in the Mn sublattice place. Al–Fe compounds or other compounds where Fe as a main component should be avoid.

An isothermal section of AM60 with variation of Fe and Mn at 500 °C, which is just below the solidify temperature, is shown in Fig. 2. An approximately phase boundary line as $y = 0.022 * (x - 0.0070)$ is observed in Fig. 2. When Fe content in final alloy does not exceed the boundary line, there will be no Al–Fe compound formed. Accordingly, no severe galvanic corrosion can happen. This value 0.022 is quite close to the experimental obtained limiting ratio of Fe/Mn as 0.021 for AM60 alloy [8]. Considering possible experimental errors for such small value, the agreement between current calculation and experimental results is excellent. Therefore, this kind of calculation can guide search of other additional elements or conditions.

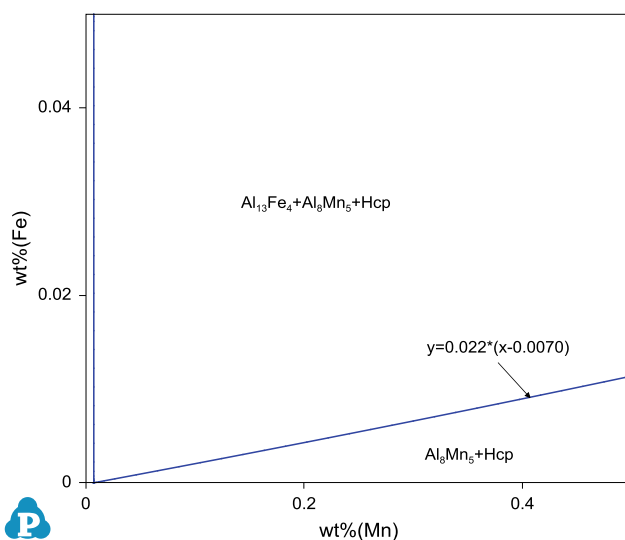


Fig. 2 Isothermal section of AM60 with variation of Fe and Mn at 500 °C [27]

It is suggested, by enclosing Fe or other impurities in some defined compounds when the impurities are not the main component, harm effect on the galvanic corrosion coming from these impurities can be reduced or even avoided. Hence, by controlling the final formed precipitates with different elements addition in Mg-alloy can control the galvanic corrosion of Mg-alloy.

Controlling Natively Formed Oxides Film on Surface of the Alloy

When contacting with air, an oxide film will instantly form on the surface of Mg alloys. The PBR is 0.81 for Mg, less than 1. For general studies, it is suggested to add another element, which have a higher value of PBR, to obtain compact protective oxides film. In this case, the formed combination of this oxide and MgO could have a PBR value above 1. However, in our experimental observation [30], Mg–Ca alloy shows better anti-oxidation property than that of Mg–Gd alloy, where the P-B value of Ca is even small than that of Mg. A structure of difference size closing packing oxides (DS-CP) film is suggested in our work [30]. As shown in Fig. 3, only with small amount Ca addition (3 wt%) in the alloy, the fraction of finally formed CaO in the oxide film is up to 80% [30]. In addition, it is shown the fraction of CaO is increasing when it is closing to the inner substrate, which means Ca can diffuse fast to the surface and be oxidized.

According to the formation energy of oxide, both Gd and Ca are more prone to be oxidized than Mg at high temperature. Hence, the oxidations and enrichments of Gd and Ca in the surface were observed. With both Ca and Gd added to

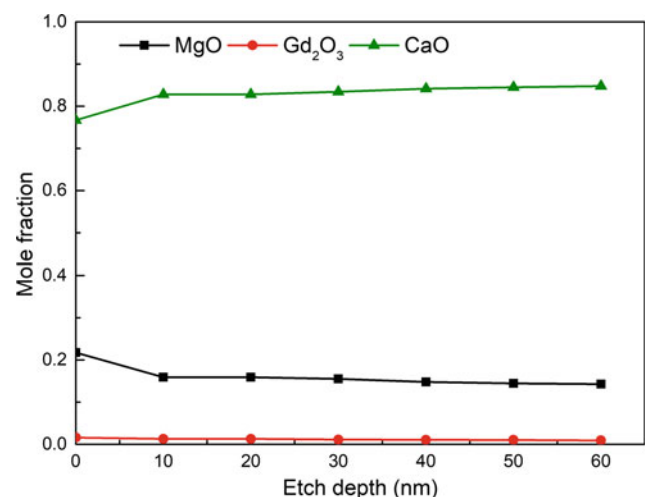


Fig. 3 Distribution of oxides in the surface of Mg–3.5Gd–0.5Ca (wt%) alloy by X-ray photoelectron spectroscopy (XPS) depth profiling [30]

Mg alloy, a phenomena of preferential oxidation of Ca and a competing diffusion kinetics between Ca and Gd was observed [30]. With Ca addition to Mg–Gd alloy, Gd_2O_3 and enrichment of Gd at the surface were disappeared. Instead, the formation of CaO and enrichment of Ca at the surface was observed, as shown in Fig. 3. A mechanism of selective oxidation resulting in competing diffusion kinetics is suggested in our work.

Based on this selective oxidation and competing diffusion kinetics mechanism, the anti-corrosion property of current commercial alloys can be improved by adding small amount defined diffuse fast elements.

Conclusion

Three alloy design strategies for native anti-corrosion Mg alloy were proposed:

- (1) Purifying of the Mg-melt by forming high-density precipitates in the settling process;
- (2) Enclosing impurities in harmless compounds by controlling the formed precipitates in the final alloy;
- (3) Controlling the composites of oxides formed on the surface by alloying defined elements to obtain passive, close packing oxides film.

Based on the above three strategies, new designed Mg alloy with better corrosion resistance property can be expected. According to our experiments and calculation, it is observed that Mn has the both purification effect and enclosing effect for the impurities [27] and Mg–Ca alloy is passive at the high temperature [30]. According to above three strategies, a broad selective of anti-corrosion Mg–X (–Y) alloy and as well, the improvement of the current commercial alloy by alloying design can be performed.

Acknowledgements The authors thank the fund from the National Key Research and Development Program of China with No. 2016YFB0301100.

References

1. Abbott TB (2015) Magnesium: Industrial and Research Developments over the last 15 years. *Corrosion* 71:120–127. <https://doi.org/10.5006/1474>
2. Mordike BL, Ebert T (2001) Magnesium Properties - applications - potential. *Mater Sci Eng A* 302:37–45. [https://doi.org/10.1016/S0921-5093\(00\)01351-4](https://doi.org/10.1016/S0921-5093(00)01351-4)
3. Wang TXJJ, Xu DK, Wu RZ, et al (2017) What is going on in magnesium alloys? *J Mater Sci Technol* 12–14. <https://doi.org/10.1016/j.jmst.2017.07.019>
4. Joost WJ, Krajewski PE (2017) Towards magnesium alloys for high-volume automotive applications. *Scr Mater* 128:107–112. <https://doi.org/10.1016/j.scriptamat.2016.07.035>
5. Brady MP, Joost WJ, Warren CD (2017) Insights from a recent meeting: Current status and future directions in magnesium corrosion research. *Corrosion* 73:452–462. <https://doi.org/10.5006/2255>
6. Song G, Atrens A (2000) Corrosion Mechanisms of Magnesium Alloys. *Adv Eng Mater* 11–33. [https://doi.org/10.1002/\(sici\)1527-2648\(199909\)11:1%3c11::aid-adem11%3e3.0.co;2-n](https://doi.org/10.1002/(sici)1527-2648(199909)11:1%3c11::aid-adem11%3e3.0.co;2-n)
7. Esmaily M, Svensson JE, Fajardo S, et al (2017) Fundamentals and advances in magnesium alloy corrosion. *Prog Mater Sci* 89:92–193. <https://doi.org/10.1016/j.pmatsci.2017.04.011>
8. Hillis JE, Reichek KN (1986) 860288 High purity magnesium AM60 alloy: the critical contaminant limits and the salt water corrosion performance. SAE Tech Pap Ser
9. Hillis JE, Shook S (1989) 890205 Composition and performance of an improved magnesium AS41 alloy. SAE Tech Pap Ser
10. Mercer WE, Hillis JE (1992) 920073 The Critical Contaminant Limits and Salt Water Corrosion Performance of Magnesium AE42 Alloy. SAE Tech Pap Ser. <https://doi.org/10.4271/920073>
11. Reichek KN, Clark KJ, Hillis JE (1985) 850417 Controlling the Salt Water Corrosion Performance of Magnesium AZ91 Alloy. SAE Tech Pap Ser. <https://doi.org/10.4271/850417>
12. Hillis J. (1983) 830523 The effects of heavy metal contamination on magnesium corrosion performance. SAE Tech Pap Ser
13. Liu M, Uggowitzer PJ, Schmutz P, Atrens A (2008) Calculated phase diagrams, iron tolerance limits, and corrosion of Mg–Al alloys. *Jom* 60:39–44. <https://doi.org/10.1007/s11837-008-0164-2>
14. Qiao Z, Shi Z, Hort N, et al (2012) Corrosion behaviour of a nominally high purity Mg ingot produced by permanent mould direct chill casting. *Corros Sci* 61:185–207. <https://doi.org/10.1016/j.corsci.2012.04.030>
15. Chen X, Pan F, Mao J (2012) CN 102672148 A, Chinese Patent
16. Chen X, Yan T, Pan F, Mao J (2015) CN 104593612 A Chinese Patent
17. Pan F, Mao J, Chen X, et al (2015) CN 104630516 A Chinese Patent
18. Prasad A, Uggowitzer PJ, Shi Z, Atrens A (2012) Production of high purity magnesium alloys by melt purification with Zr. *Adv Eng Mater* 14:477–490. <https://doi.org/10.1002/adem.201200054>
19. Parthiban GT, Palaniswamy N, Sivan V (2009) Effect of manganese addition on anode characteristics of electrolytic magnesium. *Anti-corrosion Methods Mater* 56:79–83. <https://doi.org/10.1108/00035590910940069>
20. Matsubara H, Ichige Y, Fujita K, et al (2013) Effect of impurity Fe on corrosion behavior of AM50 and AM60 magnesium alloys. *Corros Sci* 66:203–210. <https://doi.org/10.1016/j.corsci.2012.09.021>
21. Birbilis N, Williams G, Gusieva K, et al (2013) Poisoning the corrosion of magnesium. *Electrochem Commun* 34:295–298. <https://doi.org/10.1016/j.elecom.2013.07.021>
22. Liu M, Song GL (2013) Impurity control and corrosion resistance of magnesium-aluminum alloy. *Corros Sci* 77:143–150. <https://doi.org/10.1016/j.corsci.2013.07.037>
23. Pan F, Chen X, Yan T, et al (2016) A novel approach to melt purification of magnesium alloys. *J Magn Alloy* 4:8–14. <https://doi.org/10.1016/j.jma.2016.02.003>
24. Wu GH, Gao HT, Ding WJ, Zhu YP (2005) Study on mechanism of iron reduction in magnesium alloy melt. *J Mater Sci* 40:6175–6180. <https://doi.org/10.1007/s10853-005-3161-7>
25. Chen X, Pan F, Mao J (2011) CN 102296184 A Chinese Patent
26. Gao H, Wu G, Ding W, et al (2004) Study on Fe reduction in AZ91 melt by B₂O₃. *Mater Sci Eng A* 368:311–317. <https://doi.org/10.1016/j.msea.2003.11.017>
27. Yuan Yuan, Jiajia Wu, Tao Chen, Tingting Liu, Dajian Li, Xianhua Chen, Aitao Tang, Fusheng Pan (2018) The CALPHAD investigation of the Mn effect on the melt purification and Fe

- tolerance limit in AZ and AM series of Magnesium alloy, submitted
28. Abaturov IS, Popel PS, Brodova IG, et al (2008) Exploration of the viscosity temperature dependences and microstructure of magnesium-based commercial alloy AZ91D with small additions of calcium. *J Phys Conf Ser* 98:6–10. <https://doi.org/10.1088/1742-6596/98/6/062023>
 29. Simanjuntak S, Cavanaugh MK, Gandel DS, et al (2015) The Influence of Iron, Manganese, and Zirconium on the Corrosion of Magnesium : An Artificial Neural Network Approach. *corrosion* 71:199–208
 30. Jiajia Wu, Xiaowen Yu, Dajian Li, Yuan Yuan, Bin Jiang, Fusheng Pan (2018) The study of high temperature oxidation behavior of Mg-Gd and Mg-Gd-Ca Alloys, submitted